

## P-T CONDITIONS OF THE JANDAGH METAPELITIC SCHISTS, NORTHEASTERN ISFAHAN PROVINCE, IRAN

© 2010 S. M. Tabatabaei Manesh\*, M. Sharifi\*, A. Romanko\*\*

\*University of Isfahan, HezarJerib st., Isfahan, Iran, 81746–73441;  
e-mail: Tabataba@sci.ui.ac.ir

\*\* Geological Institute, Russian Academy of Sciences, Pyzhevsky per. 7, Moscow, 119017, Russia;  
e-mail: a-romanko@ya.ru

Received July 5, 2009, in final form November 25, 2009

**Abstract**—The metapelitic schists of Jandagh or simply Jandagh metapelites can be divided into four groups based on mineral assemblages: (1) quartz–muscovite schists, (2) quartz–muscovite–biotite schists, (3) garnet–muscovite–chlorite schists, and (4) garnet–muscovite–staurolite schists. The Jandagh garnet–muscovite–chlorite schists show the first appearance of garnets. These garnets contain 58–76% almandine, 1–18% spessartine, and 8–20% grossular. Microprobe analysing across the garnets demonstrates an increase in Mg# from core to rim. This is a feature of the prograde metamorphism of metapelites. Well-preserved garnet growth zoning is a sign that metapelites were rapidly cooled and later metamorphic phases had no effect here. The appearance of staurolite in garnet–muscovite–chlorite schists signifies a beginning of the amphibolite facies. The absence of zoning in staurolite suggests that its formation and growth during prograde metamorphism occurred at a widely spaced isograd. Thermobarometric investigations show that the Jandagh metapelites were formed within a temperature range of 400–670°C and pressures of 2.0–6.5 kbar. These results are in agreement with the mineral paragenetic evidence and show the development of greenschist and amphibolite facies in the area studied.

### INTRODUCTION

The Jandagh area is located in the northeast of Isfahan and is a unique field laboratory for studying regional metamorphism in Iran. This region surrounds a very large section of the southern parts of the low lying salt plain (Fig. 1).

Metapelites<sup>1</sup> are the best known metamorphic rocks of Jandagh, in which the main constituent minerals show a regular distribution pattern that may be related to the grade of metamorphism.

The first geological studies of the Jandagh region including the preparation of geological maps started in 1955. Researchers who studied the geology of Iran, such as A.F. Stahl and von Zur (1897), A. Ganser (1955), and J. Stöcklin (1968a) have made references to Jandagh. In 1975 Russian researchers made preliminary studies of the Anarak–Khur–Jandagh region (Romanko et al., 1984) and published a report in 1984

in compliance with the “Techno-Export” contract. Other studies of this region include Hafez’s M.S. thesis entitled “The Geology and Petrology of Igneous and Metamorphic Rocks of the Khur–Jandagh region (Central Iran)” (Hafez, 1996).

### METHODOLOGY AND GEOLOGY

Minerals were analysed using a Cameca electron microprobe at the Iran Center of Technological Research, and the whole rock analysis was carried out by the ICP-MS method at the Amdel Laboratory, Australia (Table 1). Also, a series of current petrologic methods such as texture and structure examination, paragenetic analysis, regional categorization of coexisting minerals based on microprobe profiles and, finally, geothermobarometrical calculations were used. In this study the main issue centered on *Ms*, *St*, *Chl*, *Grt*, *Bt* as a collection of minerals which, in the presence of H<sub>2</sub>O and *Qtz* are sensitive to the conditions of metamorphism.

### PETROGRAPHY AND MINERAL CHEMISTRY

The main purpose of this section is to characterize mineral assemblages and their compositions in the rocks from the Jandagh area and show the relationships between the minerals in different rock types. The metamorphic rocks in this area are serpentized peridotite, mylonitic granite, amphibolite, marble and alternating layers of schist, quartzite and marble (Fig. 2). The general feature of Metapelitic schists in the Jandagh area is the presence of lepidoblastic, porphy-

<sup>1</sup> The following mineral abbreviations and thermodynamic symbols are used: *Alm* – almandine; *And* – andalusite; *Ann* – annite; *Bt* – biotite; *Chl* – chlorite; *Crd* – cordierite; *En* – enstatite; *Grt* – garnet; *Grs* – grossular; *Hbl* – hornblende; *Kfs* – K-feldspar; *Ms* – muscovite; *Pl* – plagioclase; *Prp* – pyrope; *Qtz* – quartz; *Sil* – sillimanite; *St* – staurolite.

$$X_i^{Ms} = i / (Fe + Mg + Al(VI)) \quad i = Fe, Mg, Al(VI);$$

$$X_j^{Bt} = j / (Fe + Mg + Al(VI) + Ti) \quad j = Fe, Mg, Al(VI), Ti;$$

$$X_k^{Grt} = k / (Fe + Mg + Ca + Mn) \quad k = Fe, Mg, Ca, Mn;$$

$N_i = 100X_i$ ;  $a_i^\alpha$ , – activity of the component *i* of the mineral  $\alpha$ ;  
*T* – temperature, (K/C); *P* – pressure, kbar.

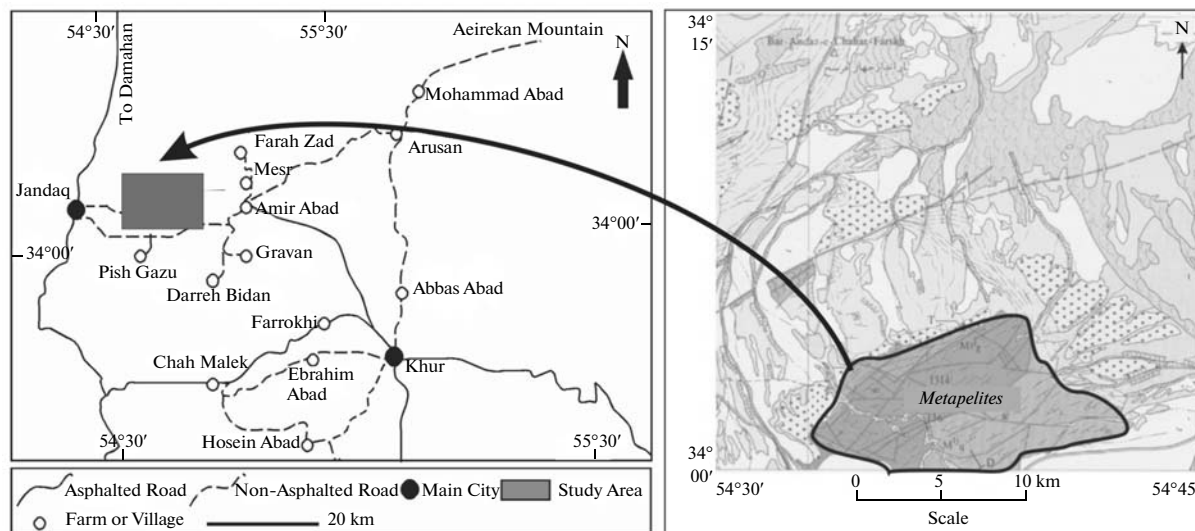


Fig. 1. Geological map of the area studied and access roads (Technoexport, 1974).

blastic, lepto-porphroblastic and lepto-porphro-poikiloblastic textures. The whole rock compositions of Jandagh Metapelites fall within the pelagic shale zone in the AFM-diagram, having higher Al and Fe and lower Ca than those of platformic shales (Fig. 3).

The *Metapelite* rocks of Jandagh are subdivided into four types:

(1) Quartz–muscovite schists ( $Qtz + Ms + Kfs + Pl$ ).

These rocks contain substantial amounts of organic matter and have very distinct lepidoblastic textures. Small grains of quartz with smooth boundaries and an average size of 0.1 to 0.2 mm and aligned muscovite sheets, 0.1 to 0.2 mm in average size, account for 95% of these rocks. The  $X_{Mg}^{Ms}$  of these rocks varies between 0.49–0.59. Biotite, chlorite and Fe oxide are the minor minerals. Muscovites embedded in opaque minerals are sometimes present in these rocks. The presence of very fine crenulations is another feature in the structures of these rocks (Fig. 4).

(2) Quartz–muscovite–biotite schists ( $Grt + Qtz + Bt + Ms + Kfs + Pl$ ) have larger grains in comparison with the quartz–muscovite schists and are not often seen as layers enriched in quartz, muscovite, and biotite accompanied by organic matter (Fig. 4). Lepidoblastic textures are a distinct feature of these rocks. Their essential minerals are grains of smooth surfaced quartz with an average size of 0.1 to 0.2 mm and aligned muscovite and biotite sheets with an average size of 0.1–0.2 mm. The simultaneous formation of these two minerals indicates reaction (1)  $Chl + Kfs = Bt + Ms + Qtz + H_2O$ . Chlorite, garnet and Fe oxide are the accessory minerals. The  $X_{Mg}^{Ms}$  varies from 0.41 to 0.54 in these rocks.

(3) Garnet–muscovite–chlorite schists ( $Grt + Qtz + Ms + Kfs + Pl + Chl$ ) have much less biotite

(about 2 to 3%) but more garnet (about 10%) in comparison with the previous group. Garnet forms irregular broken phenocrysts surrounded by smaller grains of garnet scattered within the rock (Fig. 4). Its  $X_{Mg}^{Grt}$  varies between 0.4 and 0.2, and the end member composition is as follows: almandine from 59 to 76%, spessartine from 1 to 18%, and grossular from 8 to 20%. The mineral assemblage of these rocks and the presence of muscovite and, sometimes, biotite inclusions in the garnet show that chemical reaction (2)  $Ms + Bt + Qtz = Grt + Kfs + H_2O$  has taken place. The presence of a very fine crenulation fabric is another feature in the make-up of these rocks. The  $X_{Mg}^{Bt}$  varies from 0.41 to 0.46. Figure 5 shows the position of *Bt* and *Grt* in the AFM-diagram compared with the whole rock composition. Large cores of *Grt* contain more Mg in comparison with small *Grt*, and this shows that they must have formed after prograde metamorphism; this difference is clearly evident in the AFM-diagram.

The microprobe profile of *Grt* in contact with *Chl* shows an increase in  $N_{Mg}$  near *Chl*. This is important because the  $N_{Mg}$  of *Chl* during prograde metamorphism is always higher than that of adjacent *Grt*; therefore, this observation may signify limited stability of Fe-chlorite and an increase in the amount of *Grt* and accompanying Mg-chlorite (Fig. 6 and Tabatabaei Manesh, 2006).

(4) Garnet–muscovite–staurolite schists ( $Grt + Qtz + St + Bt + Ms + Kfs + Pl + Chl$ ) have coarse grains; the matrix is composed of layers rich in *Ms* accompanied by very small amounts of *Bt* with lepidoblastic, porphyroblastic, and poikiloblastic textures. The  $X_{Mg}^{Ms}$  in these rocks varies from 0.39 to 0.60. The *Grt* present in the staurolite schists are both small and large in size, with large *Grt* containing more Mg com-

**Table 1.** Selected microprobe analyses of the schist minerals, wt %

Component	Sample Mjc11					Sample JM5d					
	<i>Grt</i>	<i>Grt</i>	<i>Grt</i>	<i>Grt</i>	<i>Grt</i>	<i>Grt</i>	<i>Grt</i>	<i>Grt</i>	<i>Grt</i>	<i>Grt</i>	<i>Grt</i>
	1	2	3	4	5	1	2	3	4	5	6
SiO <sub>2</sub>	38.534	38.363	38.867	38.653	38.113	38.14	38.23	37.86	37.74	38.30	38.38
TiO <sub>2</sub>	0.11	0.08	0.09	0.08	0.14	0.08	0.07	0.04	0.09	0.14	0.11
Al <sub>2</sub> O <sub>3</sub>	20.88	20.71	21.10	20.55	20.91	21.53	20.78	21.07	21.05	21.07	21.12
Cr <sub>2</sub> O <sub>3</sub>	0.00	0.03	0.00	0.00	0.04	0.05	0.00	0.00	0.02	0.01	0.00
FeO	25.96	24.63	28.50	32.31	32.92	31.36	31.50	33.80	32.21	31.82	30.78
MnO	6.12	7.32	2.65	0.35	0.37	0.29	0.27	0.00	0.31	0.48	0.17
MgO	0.84	0.96	1.50	1.71	2.70	1.81	1.67	4.07	1.64	1.66	2.87
CaO	6.45	6.74	6.72	5.16	4.10	6.99	7.23	2.97	7.21	7.25	7.18
Na <sub>2</sub> O	0.00	0.00	0.00	0.00	0.00	0.00	0.00	0.00	0.00	0.00	0.00
K <sub>2</sub> O	0.00	0.00	0.00	0.00	0.00	0.00	0.00	0.00	0.00	0.00	0.00
<i>Cation ratios calculated per 12 oxygens</i>						<i>Cation ratios calculated per 12 oxygens</i>					
Si	3.10	3.09	3.10	3.11	3.05	3.03	3.06	3.02	3.02	3.04	3.03
Al	1.98	1.97	1.98	1.95	1.97	2.01	1.96	1.98	1.98	1.97	1.96
Al(IV)	0.00	0.00	0.00	0.00	0.00	0.00	0.00	0.00	0.00	0.00	0.00
Al(VI)	1.98	1.97	1.98	1.95	1.97	2.01	1.96	1.98	1.98	1.97	1.96
Cr	0.00	0.00	0.00	0.00	0.00	0.00	0.00	0.00	0.00	0.00	0.00
Ti	0.01	0.00	0.01	0.00	0.01	0.00	0.00	0.00	0.01	0.01	0.01
Fe <sup>3+</sup>	0.00	0.00	0.00	0.00	0.00	0.00	0.00	0.00	0.00	0.00	0.00
Fe <sup>2+</sup>	1.75	1.66	1.90	2.17	2.20	2.08	2.11	2.25	2.15	2.11	2.03
Mn	0.42	0.50	0.18	0.02	0.03	0.02	0.02	0.00	0.02	0.03	0.01
Mg	0.10	0.11	0.18	0.20	0.32	0.21	0.20	0.48	0.19	0.20	0.34
Ca	0.56	0.58	0.57	0.45	0.36	0.59	0.62	0.25	0.62	0.62	0.61
Na	0.00	0.00	0.00	0.00	0.00	0.00	0.00	0.00	0.00	0.00	0.00
K	0.00	0.00	0.00	0.00	0.00	0.00	0.00	0.00	0.00	0.00	0.00
X <sub>Mg</sub>	0.04	0.05	0.08	0.09	0.13	0.09	0.09	0.18	0.08	0.08	0.14
X <sub>Ca</sub>	0.20	0.20	0.20	0.16	0.12	0.20	0.21	0.08	0.21	0.21	0.20
<i>Alm</i>	0.62	0.58	0.67	0.76	0.76	0.72	0.72	0.75	0.72	0.71	0.68
<i>Sps</i>	0.15	0.18	0.06	0.01	0.01	0.01	0.01	0.00	0.01	0.01	0.00
<i>Prp</i>	0.04	0.04	0.06	0.07	0.11	0.07	0.07	0.16	0.07	0.07	0.11
<i>Grs</i>	0.20	0.20	0.20	0.16	0.12	0.20	0.21	0.08	0.21	0.21	0.20
Component	Sample Mjc11					Sample JM5d					
	<i>Ms</i>	<i>Ms</i>	<i>Ms</i>	<i>Ms</i>	<i>Ms</i>	<i>Ms</i>	<i>Ms</i>	<i>Ms</i>	<i>Ms</i>	<i>Ms</i>	
	1	2	3	4	5	6	1	2	3	4	5
SiO <sub>2</sub>	47.85	47.08	47.74	46.89	47.69	47.49	47.37	48.55	47.04	46.85	48.17
TiO <sub>2</sub>	0.30	0.43	0.25	0.22	0.35	0.34	0.40	0.38	0.20	0.23	0.04
Al <sub>2</sub> O <sub>3</sub>	33.96	34.63	33.00	32.58	35.00	35.10	34.98	34.88	33.86	33.94	33.44
Cr <sub>2</sub> O <sub>3</sub>	0.00	0.00	0.00	0.00	0.00	0.00					
FeO	1.72	1.50	1.91	2.83	1.30	1.40	1.09	1.10	1.74	1.61	2.62
MnO	0.00	0.00	0.00	0.01	0.00	0.03	0.00	0.04	0.00	0.01	0.00
MgO	1.13	0.86	1.15	1.09	0.70	0.81	0.93	0.90	0.80	0.97	0.95
CaO	0.15	0.03	0.04	0.00	0.00	0.04	0.03	0.00	0.10	0.14	0.01

Table 1. (Contd.)

Component	Sample Mjc11						Sample JM5d					
	<i>Ms</i>	<i>Ms</i>	<i>Ms</i>	<i>Ms</i>	<i>Ms</i>	<i>Ms</i>	<i>Ms</i>	<i>Ms</i>	<i>Ms</i>	<i>Ms</i>		
	1	2	3	4	5	6	1	2	3	4	5	
Na <sub>2</sub> O	1.34	0.88	0.72	0.68	0.90	0.87	0.74	0.68	0.43	0.77	0.35	
K <sub>2</sub> O	9.46	8.82	9.21	9.86	8.70	9.00	8.48	7.99	9.55	10.52	9.80	
	<i>Cation ratios calculated per 11 oxigens</i>						<i>Cation ratios calculated per 11 oxigens</i>					
Si	3.16	3.14	3.20	3.17	3.15	3.14	3.17	3.19	3.16	3.13	3.20	
Al	2.64	2.72	2.61	2.60	2.73	2.73	2.71	2.70	2.68	2.68	2.62	
Cr	0.00	0.00	0.00	0.00	0.00	0.00	0.00	0.00	0.00	0.00	0.00	
Ti	0.01	0.02	0.01	0.01	0.02	0.02	0.02	0.02	0.01	0.01	0.00	
Fe <sup>2+</sup>	0.09	0.08	0.11	0.16	0.07	0.08	0.06	0.06	0.10	0.09	0.15	
Mn	0.00	0.00	0.00	0.00	0.00	0.00	0.00	0.00	0.00	0.00	0.00	
Mg	0.11	0.09	0.12	0.11	0.07	0.08	0.09	0.09	0.08	0.10	0.09	
Ba	0.00	0.00	0.00	0.00	0.00	0.00	0.00	0.00	0.00	0.00	0.00	
Ca	0.01	0.00	0.00	0.00	0.00	0.00	0.00	0.00	0.01	0.01	0.00	
Na	0.17	0.11	0.09	0.09	0.12	0.11	0.09	0.09	0.06	0.10	0.05	
K	0.80	0.75	0.79	0.85	0.73	0.76	0.71	0.67	0.82	0.90	0.73	
Total	6.99	6.91	6.92	6.99	6.89	6.92	6.86	6.82	6.92	7.02	6.93	
X <sub>Mg</sub>	0.54	0.50	0.52	0.41	0.49	0.51	0.60	0.59	0.45	0.52	0.39	
Component	Sample JM5d						Component	Sample Mjc11				
	<i>St</i>	<i>St</i>	<i>St</i>	<i>St</i>	<i>St</i>	<i>St</i>		<i>Bt</i>	<i>Bt</i>	<i>Bt</i>	<i>Bt</i>	<i>Bt</i>
	1	2	3	4	5	6		1	2	3	4	5
SiO <sub>2</sub>	29.01	28.69	28.55	28.57	28.71	26.39	SiO <sub>2</sub>	34.85	35.20	35.93	35.04	34.97
TiO <sub>2</sub>	0.63	0.53	0.59	0.60	0.79	1.53	TiO <sub>2</sub>	1.49	1.53	1.60	1.45	1.54
Al <sub>2</sub> O <sub>3</sub>	53.84	52.87	54.32	53.49	53.70	53.12	Al <sub>2</sub> O <sub>3</sub>	17.47	17.53	17.50	17.05	17.85
Cr <sub>2</sub> O <sub>3</sub>	0.00	0.00	0.00	0.00	0.00	0.00	Cr <sub>2</sub> O <sub>3</sub>	0.03	0.00	0.04	0.01	0.11
FeO	12.46	12.22	12.55	12.18	12.28	11.31	FeO	20.72	20.96	20.47	22.68	21.74
MnO	0.00	0.08	0.11	0.07	0.00	0.04	MnO	0.12	0.10	0.10	0.07	0.08
MgO	0.93	0.90	0.86	0.86	0.24	0.81	MgO	9.85	9.78	9.53	8.88	8.95
CaO	0.00	0.00	0.00	0.00	0.00	0.00	CaO	0.31	0.04	0.17	0.11	0.08
Na <sub>2</sub> O	0.00	0.00	0.00	0.00	0.00	0.00	Na <sub>2</sub> O	0.16	0.23	0.21	0.21	0.21
K <sub>2</sub> O	0.00	0.00	0.00	0.00	0.00	0.00	K <sub>2</sub> O	9.56	8.97	9.33	9.16	9.26
	<i>Cation ratios calculated per 46 oxigens</i>						<i>Cation ratios calculated per 22 oxigens</i>					
Si	7.99	8.03	7.87	7.95	7.98	7.91	Si	5.42	5.46	5.53	5.47	5.43
Al	17.47	17.44	17.54	17.55	17.59	17.45	Al	3.20	3.20	3.17	3.14	3.27
Cr	0.00	0.00	0.00	0.00	0.00	0.00	Cr	0.00	0.00	0.00	0.01	0.01
Ti	0.13	0.11	0.12	0.13	0.16	0.32	Ti	0.17	0.18	0.19	0.17	0.18
Fe <sup>2+</sup>	2.87	2.86	2.89	2.84	2.85	2.64	Fe <sup>2+</sup>	2.69	2.72	2.63	2.96	2.82
Mn	0.00	0.02	0.02	0.02	0.00	0.01	Mn	0.02	0.01	0.01	0.01	0.01
Mg	0.38	0.38	0.35	0.35	0.10	0.33	Mg	2.28	2.26	2.18	2.07	2.07
Ca	0.00	0.00	0.00	0.00	0.00	0.00	Ba	0.00	0.00	0.00	0.00	0.00
Zn	0.32	0.30	0.28	0.30	0.36	0.37	Ca	0.05	0.01	0.03	0.02	0.01
Na	0.00	0.00	0.00	0.00	0.00	0.00	Na	0.05	0.07	0.06	0.06	0.06
K	0.00	0.00	0.00	0.00	0.00	0.00	K	1.90	1.77	1.83	1.82	1.83
X <sub>Mg</sub>	0.12	0.12	0.11	0.11	0.03	0.11	X <sub>Mg</sub>	0.46	0.45	0.45	0.41	0.42

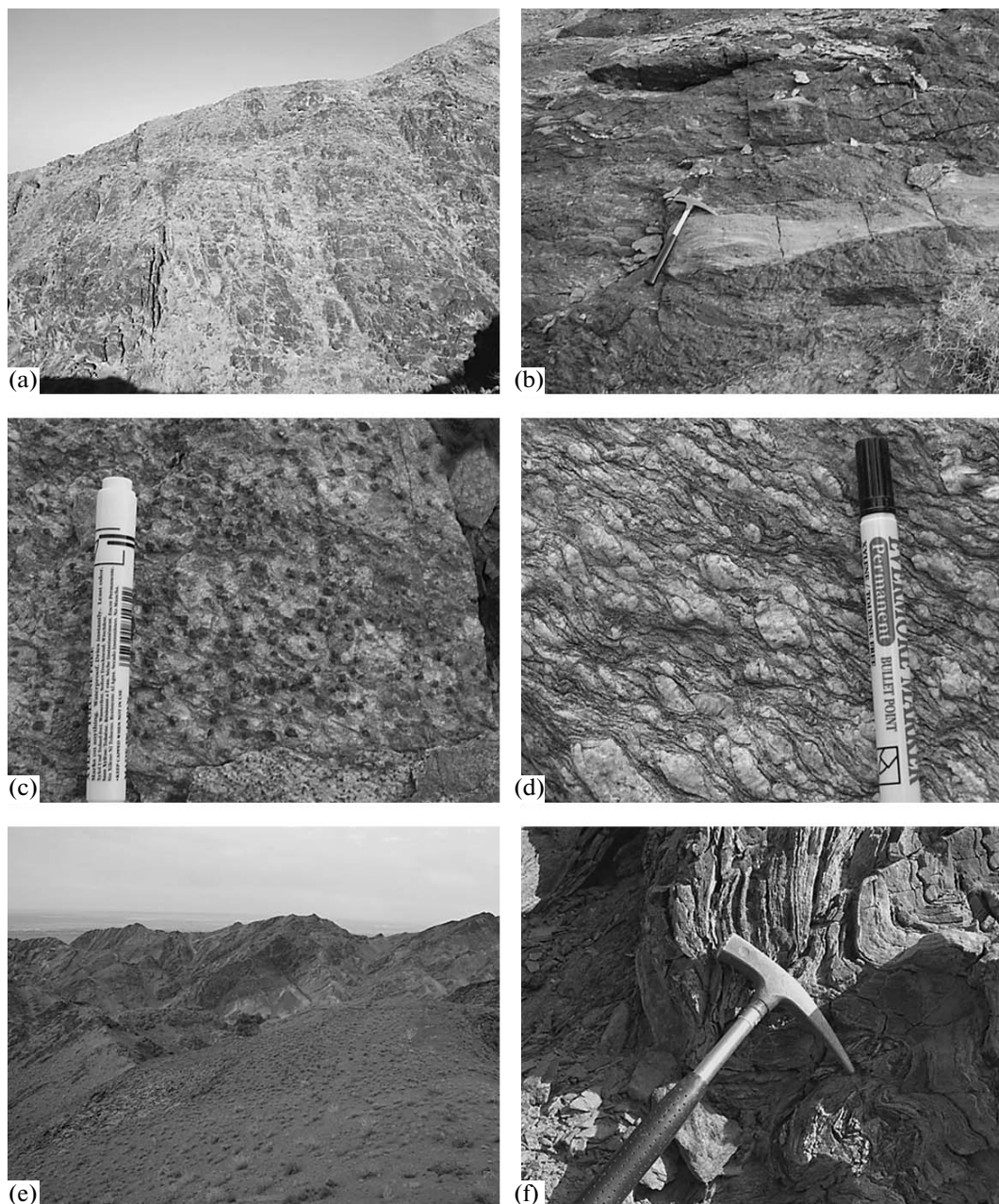


**Fig. 2.** Frontal view of Jandagh metamorphic rocks (hereafter, figures are labeled from right to left as in Persian) (a) Serpentine peridotite in the Jandagh Talc mine. (b) The alternate assurance of schist and marble in the Safahoo farm region. (c) Garnet-mica schists in the Chah-Zard region. (d) Mylonitic granites in the Safahoo farm region – a frontal view of Garnet-mica schists (picture front) and amphibolites (dark areas) in the Chah-Zard region. (e) Folding within the schists of the Safahoo farm region.

pared with small ones; this difference is clearly seen in the AFM-diagram (Fig. 7).

Broken and shapeless *Grt* with a maximum diameter of one centimeter which are typically chloritized along broken edges have integrated primary *Chl*.

The  $N_{Mg}^{Grt}$  varies between 8 and 18, and the percentages of garnet end members are from 68 to 75% almandine, 0 to 1% spessartine, 8 to 21% grossular, and 7 to 16% pyrope (Fig. 8).

Relatively intact staurolites with a diameter between 0.1 and 2.0 mm constitute approximately 6–7% of the garnet-muscovite–staurolite schists. The  $X_{Mg}^{St}$  varies from 0.3 to 0.12. The appearance of staurolite in metapelites starts at an approximate temperature of 500°C and signifies the beginning of the amphibolite facies (Masoudi et al., 2006). The absence of zoning in the staurolite from the schists (Fig. 7) suggests the formation and growth of this mineral during prograde

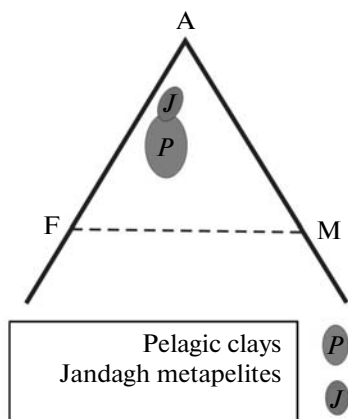


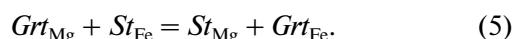
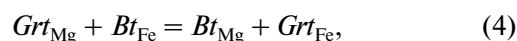
Fig. 3. Composition of Jandagh Metapelitic rocks in the AFM-diagram (Bucher et al., 2002).

metamorphism occurring at a widely spaced isograde. The presence of the assemblage *Grt* + *St* + *Chl* + *Bt* signifies that the reaction  $Grt + Chl = St + Bt$  has taken place, and almost all *Bt* of these rocks (4–5%) is due to this reaction.

#### THE THERMODYNAMIC CONDITION OF LOCAL MINERAL EQUILIBRIUM

Metamorphic reactions, including net-transfer and exchange reactions, provide insight into the *P-T* conditions of metamorphism. To gain information in this

respect, it is necessary to analyze the minerals involved in these reactions. In order to calculate the thermodynamic parameters of mineral equilibrium, the Geo-Path data bank was used (Perchuk et al., 1992). The well-preserved growth zoning in the *Grt* of the rocks shows an increase in Fe and Mn and a decrease in Mg from core to rim. This suggests that the staurolite schists of Jandagh were formed under amphibolite facies conditions and prior to their homogenization have endured metamorphism of the higher amphibolite facies (Perchuk et al., 2007). Given the coexistence of *Grt* and *St* and also *Grt* and *Bt*, the following exchange reactions were used as thermometers:



The microprobe analysis of *Bt*, *Ms*, *Grt* from the mineral assemblage  $Qtz + Grt + Qtz + Ms + Kfs + Bt$  shows a state of equilibrium in the reaction:  $Ms + Bt + Qtz = Grt + Kfs + H_2O$ , which was used as a barometer (Perchuk, 1990). The results of the geothermobarometry of these rocks on the basis of the Geo-Path data bank are shown in Tables 2–4.

The thermobarometric study of Jandagh metapelites allowed us to obtain their metamorphic conditions within temperatures from 400 to 670°C and pressures from 2 to 6.5 kbar. The *P-T* path of metamorphism is illustrated on Fig. 9. These results are consistent with the paragenetic evidence.

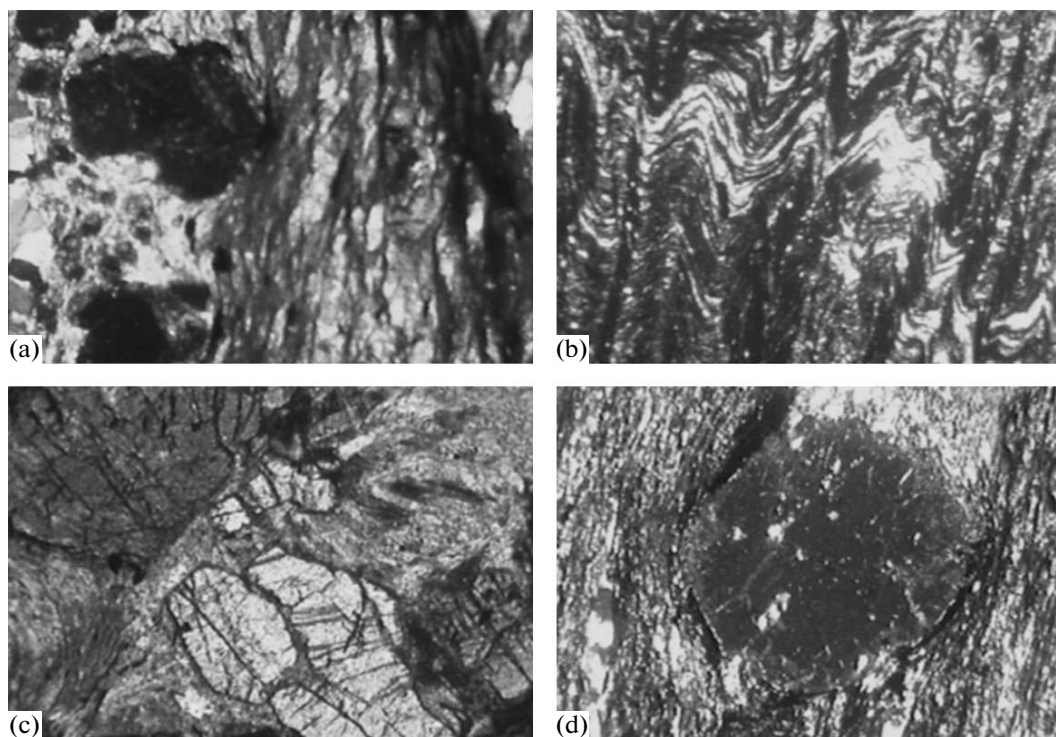


Fig. 4. View of the Jandagh schists. (a) Garnet–muscovite schist, (b) quartz–muscovite schist, (c) garnet–muscovite–staurolite schist, (d) garnet–muscovite–chlorite schist (all pictures taken with XPL light; magnification × 40).

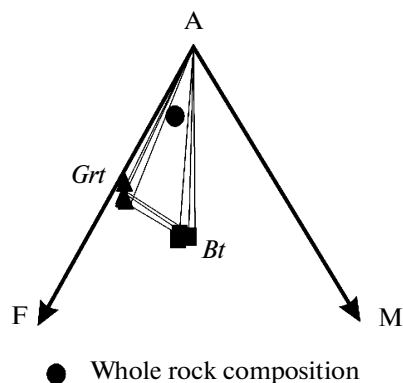


Fig. 5. Position of *Grt* and *Bt* in the paragenetic AFM-diagram. Whole rock composition was also included for comparison (Bucher et al., 2002).

### CONCLUSIONS

The study of Jandagh metapelitic rocks shows that these rocks can be divided into four categories based on mineral assemblages: quartz–muscovite, quartz–muscovite–biotite, garnet–muscovite–chlorite, and garnet–muscovite–staurolite schists.

In the quartz–muscovite–biotite schists the *Ms* + *Bt* assemblage replaced *Chl* + *Kfs* via the net-transfer reaction  $Chl + Kfs = Bt + Ms + Qtz + H_2O$ . The Jandagh garnet–muscovite–chlorite schists show the first appearance of *Grt* cores. These garnets are basically composed of 58–76% almandine, 1–18% spessartine, and 8–20% grossular after the net-transfer reaction  $Ms + Bt + Qtz = Grt + Kfs + H_2O$ .

The microprobe analysis along *Grt* in Jandagh metapelites rocks shows that the Mg number of garnets varies and increases from core to rim. This is a feature of the prograde metamorphism of metapelitic rocks. The well-preserved garnet growth zoning is a sign that metapelites were rapidly cooled and later metamorphic processes had no effect on them.

The appearance of staurolite in the garnet–muscovite–chlorite schists signifies the beginning of amphibolite facies. The absence of zoning in staurolite from these schists suggests that the formation and growth of this mineral occurred during prograde metamorphism at a widely spaced isograd.

The presence of the *Grt* + *St* + *Chl* + *Bt* assemblage shows that the formation of staurolite occurred via the net-transfer reaction  $Grt + Chl = St + Bt$ . Thermobarometric

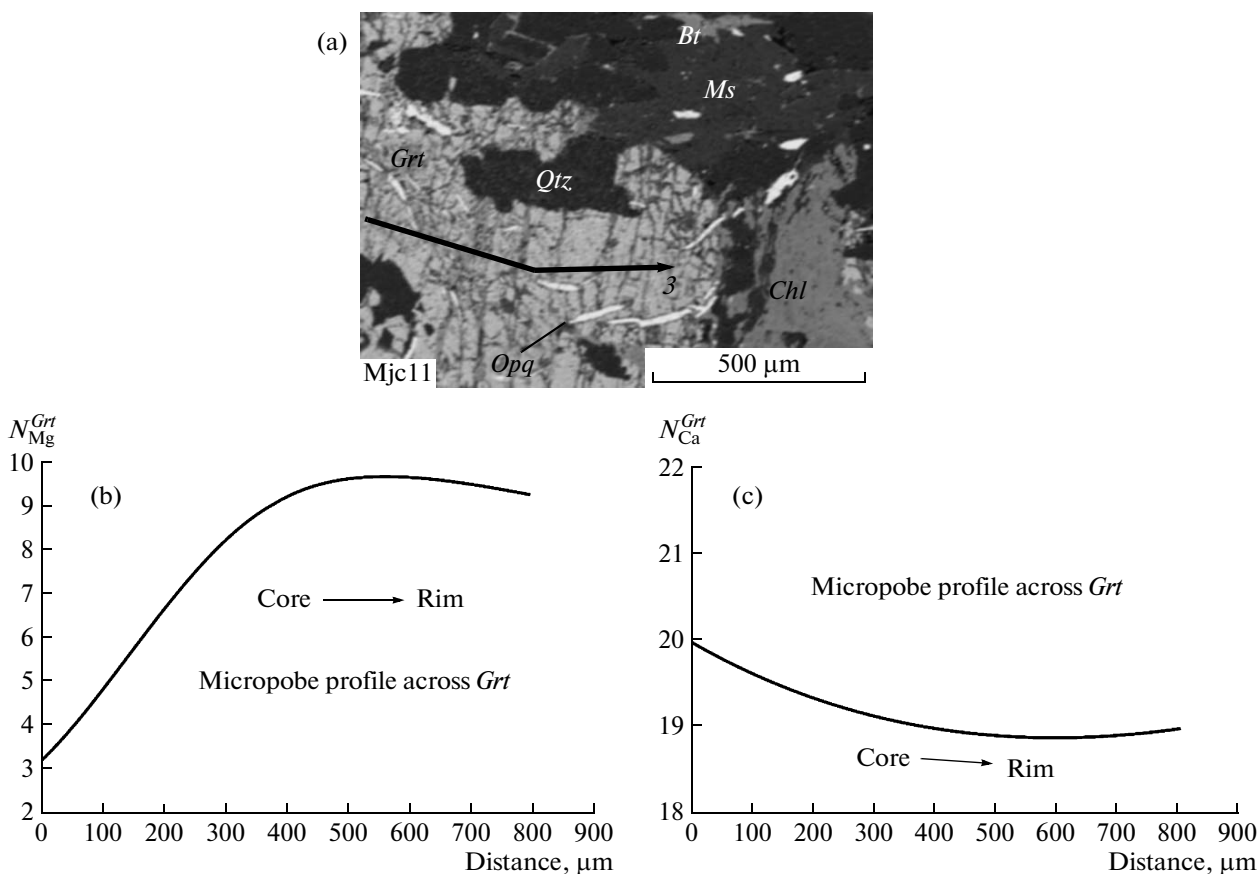


Fig. 6. (a) The BSI (back scattered image) of *Grt* and adjacent *Chl* in a sample of Jandagh metapelites, (b) and (c): the profile of Mg and Ca in the *Grt* in contact with *Chl*.

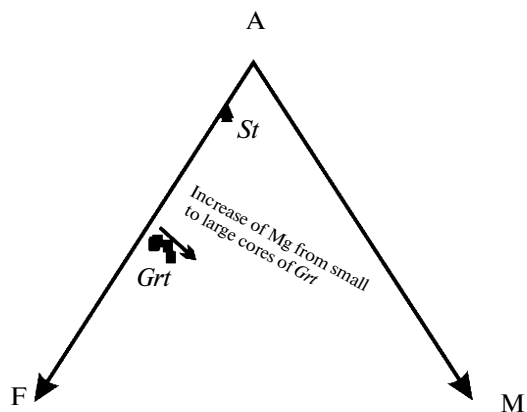


Fig. 7. Location of staurolite on the AFM-diagram. It is clearly seen that there is an increase of Mg from small to large *Grt* cores.

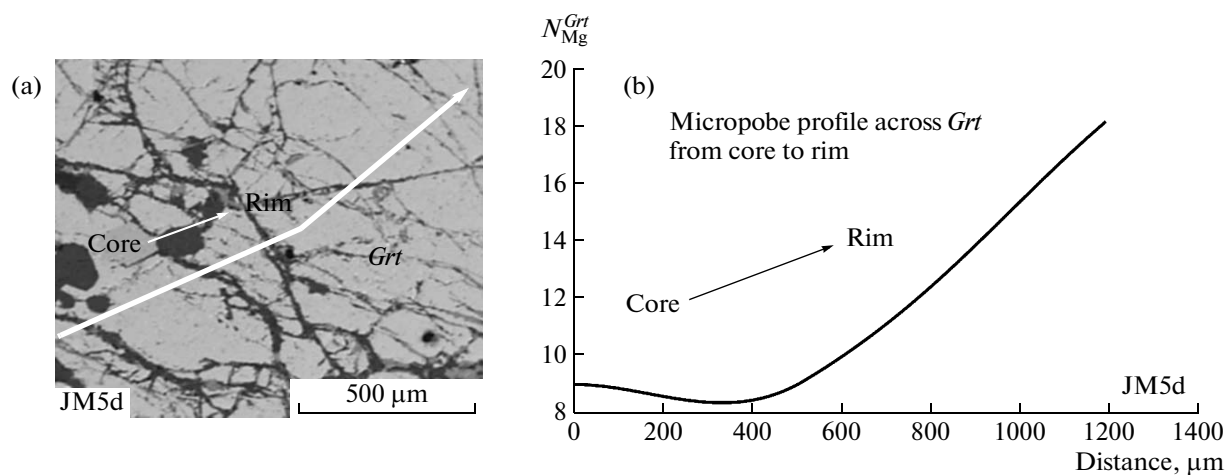


Fig. 8. (a) BSI of *Grt* in Jandagh metapelites, (b) the profile of *Grt* from core to rim.

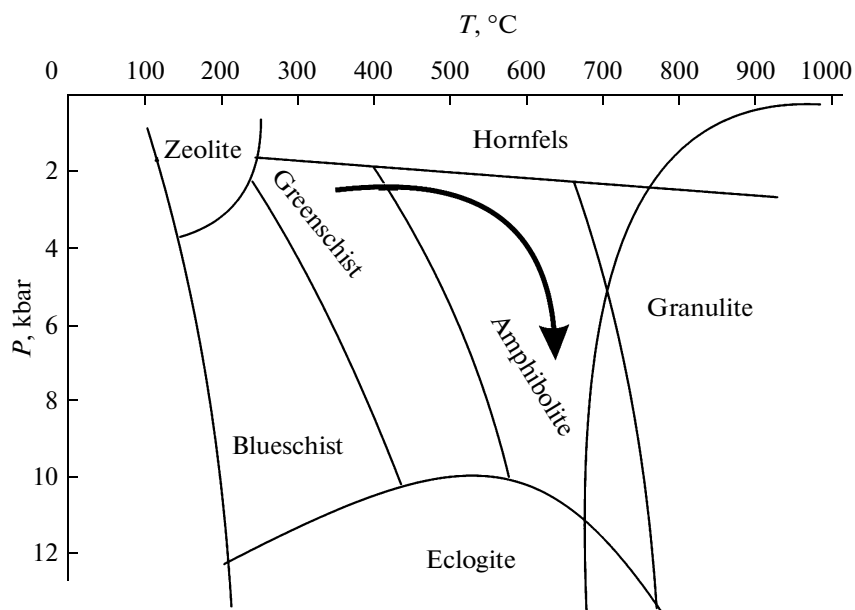


Fig. 9. Metamorphic path of the Jandagh metapelites on the facies diagram (Yardley, 1990).



**Table 2.** Temperature calculation results for the four *Grt + St* assemblages in Jandagh metapelites based on reaction (5)

$X_{Mg}^{St}$	$X_{Mg}^{Grt}$	Temperature, °C
0.12	0.09	611
0.12	0.09	617
0.11	0.08	614
0.03	0.08	670

**Table 3.** Temperature calculation results for the five *Grt + Bt* assemblages in Jandagh metapelites based on reaction (4)

$X_{Mg}^{Bt}$	$X_{Mg}^{Grt}$	Temperature, °C
0.46	0.04	408
0.45	0.05	429
0.45	0.08	495
0.41	0.08	534
0.42	0.13	606

**Table 4.** *P-T* parameters for the five *Grt + Bt + Ms + Qtz* assemblages in Jandagh metapelites

$X_{Mg}^{Bt}$	$X_{Mg}^{Grt}$	$X_{Al}^{Ms}$	$X_{Mg}^{Ms}$	<i>P</i> , kbar*	<i>T</i> , °C**
0.46	0.04	0.93	0.54	2.04	442
0.45	0.05	0.94	0.50	2.17	518
0.45	0.08	0.92	0.52	3.94	564
0.41	0.09	0.91	0.41	5.86	552
0.42	0.13	0.95	0.49	6.4	626

\* Pressure calculated on the basis of reaction (2).

\*\* Temperature calculated on the basis of reaction (4).

estimates based on the above reactions show that Jandagh metapelites were formed within a temperature range of 400–670°C and a pressure range of 2.0–6.5 kbar. These results are consistent with the examination of mineral assemblages and show the effect of metamorphism of the Jandagh pelitic sediments under greenschist and amphibolite facies conditions.

#### ACKNOWLEDGMENTS

This research is a part of the studies related to project 850708, which was sponsored by Isfahan University's Department of Research and Technology, to which we offer our sincere appreciation.

#### REFERENCES

1. *Bucher K., Frey M.* Petrogenesis of Metamorphic Rocks. Berlin, Heidelberg, New York, Springer-Verlag, 7th ed., 2002.
2. *Ganser A.* New Aspects of Geology in Central Iran (With Discussion), World Petrol. Congress. 4th Section 1. 1955. P. 278–300.
3. *Hatef M.* Geology and Petrology of Igneous and Metamorphic Rocks in Khur-Jandagh Region (Central Iran): Thesis. Isfahan University, 1996.
4. *Masoudi F.B., Mehrabim B., Mahmoudi Sh.* Garnet (Almandine-Spessartine) Growth Zoning and Its Application to Constrain Metamorphic History in Dehsalm Complex, Iran // *J. Sci. I.R. Iran.* 2006. V. 17. № 3. P. 235–244.
5. *Perchuk L.L.* Derivation of Thermodynamically Consistent System of Geothermometers and Geobarometers for Metamorphic and Magmatic Rocks // *Progress in Metamorphic and Magmatic Petrology*, Cambridge University Press, 1990. P. 93–112.
6. *Perchuk L.L., Podladchikov Yu.Yu., Polaykov A.N.* PT-Paths and Geodynamic Modeling of Some Metamorphic Processes // *J. Metamorph. Geol.* 1992. V. 10. P. 311–319.
7. *Perchuk L.L., van Reenen D.D., Smith C.A., Vankal D.A., Boshoff R., Varlamonov S.M., Tabatabaei Manesh S.M.* Isobaric Heating Recorded in Polymetamorphic Rocks from the Central Zone of the Limpopo High-Grade Terrain, South Africa // *Lithos.* 2008. V. 103. P. 70–105.
8. *Romanko E., Kokorin Y.U., Krivyakin B., Susov M., Morozov L., Sharkovski M.* Outline of Metallogeny of Anarak Area (Central Iran), Ministry of Mines and Metals // Geological Survey of Iran, V / O Technoexport. 1984. 136 p.
9. *Stah A.F., von Zur.* Geologie von Persian Geognostische Beschreibung des Nordlichen und Zentral-Persiens // *Petermanns Mitt.* 1897. № 122. P. 1–72.
10. *Stöcklin J.* Structural History and Tectonics of Iran // *Rev. Amer. Assoc. Petrol. Geol.* B. 1968. V. 52. № 7. P. 1229–1258.
11. *Tabatabaei Manesh S. M.* Petrology of polymetamorphic rocks in the Central zone of the Limpopo high-grade terrain, South Africa: Ph. D. Thesis. Moscow State University, 2006. 184 p.
12. Technoexport, Geology of Jandagh Area (Central Iran) // Geological Survey of Iran, V / O Technoexport. Report 4. 1974. 96 p.
13. *Yardley B.W.D.* An Introduction to Metamorphic Petrology. Longman Scientific & Technical, Singapore, 2nd edition, 1990. 248 p.